ELSEVIER

Thermochimica Acta 395 (2003) 191–200

thermochimica acta

www.elsevier.com/locate/tca

Wax appearance temperatures of vegetable oils determined by differential scanning calorimetry: effect of triacylglycerol structure and its modification☆

A. Adhvaryu[a,b], S.Z. Erhan[b,*], J.M. Perez[a]

[a]*Department of Chemical Engineering, Pennsylvania State University, University Park, PA 16802, USA*
[b]*USDA/NCAUR/ARS, Food and Industrial Oil Research, 1815 N. University Street, Peoria, IL 61604, USA*

Received 19 November 2001; received in revised form 6 March 2002; accepted 9 March 2002

Abstract

Crystallization and wax appearance temperatures of a series of vegetable oils (natural, genetically and chemically modified) were studied using differential scanning calorimetry (DSC). The fatty acid chains of a triacylglycerol molecule have a bend 'tuning fork' conformation and undergo molecular stacking during the cooling process. Wax crystallization at low temperature is controlled by steric and geometrical constrains in these molecules. This study describes an approach to quantify and predict wax appearance temperature of vegetable oils based on the statistical analysis of DSC and NMR data. A molecular modeling program was used to design triacylglycerol molecules with different fatty acid (e.g. oleic and linoleic) chains to illustrate their effect on the crystallization process. Effect of pour point depressant (PPD) additives on vegetable oil crystallization is also discussed. Published by Elsevier Science B.V.

Keywords: DSC; Vegetable oils; Wax formation; NMR; Molecular modeling; Statistical analysis

1. Introduction

Vegetable oils when subjected to low temperature environment undergo solidification through crystallization and therefore are a major hurdle for use in industrial applications. The relatively poor low temperature flow properties of vegetable oils arise from the appearance of waxy crystals that rapidly agglomerate resulting in the solidification of the oil. Vegetable oil is a complex molecular system and therefore the transition from liquid to solid state do not occur at a particular temperature, but over a wide temperature range involving several polymorphic forms (α, β', β) [1–3] contributing to the wax appearance and crystallization process. This deposition of waxy materials from oil results in a rapid viscosity increase leading to poor pumpability, lubrication and rheological behavior.

Several standard methods are currently available for determining the low temperature properties of vegetable oils, such as pour point (ASTM D-97) and cloud point (ASTM D-2500). These methods are extremely time consuming and data reproducibility between laboratories is poor. Differential scanning calorimetry (DSC) is a relatively simple and reproducible technique capable of providing a direct measurement of the

☆ Names are necessary to report factually on available data; however, the USDA neither guarantees nor warrants the standard of the product, and the use of the name by USDA implies no approval of the product to the exclusion of others that may also be suitable.

* Corresponding author. Tel.: +1-309-681-6532; fax: +1-309-681-6340.
E-mail address: erhansz@ncaur.usda.gov (S.Z. Erhan).

0040-6031/02/$ – see front matter. Published by Elsevier Science B.V.
PII: S0040-6031(02)00180-6

ΔH (change in enthalpy) for a system undergoing physical and chemical changes during heating or cooling [4–6]. A number of studies have been carried out on the cooling behavior of different wax bearing crudes and mineral base oils using DSC [7–12]. Reports are also available on the application of DSC for identification of various stable polymorphs in pure single acid triacylglycerol structure by heating and cooling experiments ([13–15] and references therein). However the situation in an unmodified or genetically modified vegetable oil is far more complex. This is primarily due to the presence of different fatty acid moieties, their chain length, abundance, structural difference and configuration in the triacylglycerol that makes vegetable oils significantly different from other pure molecules. All the above factors individually and collectively are capable of influencing the physical properties of vegetable oils.

In this paper we describe the application of DSC to determine wax appearance and crystallization temperature in different vegetable oils. The effect of fatty acid composition, structure and spatial orientation on cooling process is discussed. A molecular modeling program was used to design different triacylglycerol molecules using an energy minimization approach. The results were used to explain the stacking process of the 'tuning fork' structure and wax appearance temperature of vegetable oils. The usefulness of statistical models based on structural data derived from proton nuclear magnetic resonance (^{1}H NMR), for the prediction of low temperature crystallization of vegetable oils is also discussed.

2. Experimental

2.1. Materials

The vegetable oils used in the study were cotton seed, corn (local grocery store), sunflower (sunflr), safflower (saflr) (Liberty Vegetable Oil, CA), soybean oil (SBO) (Pioneer Hi Bred Intl., IA). The genetically modified vegetable oils were high oleic sunflower (HO sunflr) (Intl. Flora Tech, Gilbert, AZ), high oleic safflower (HO saflr) and high linoleic safflower (HL saflr) oil (Oil Seeds Intl., CA). The chemically modified oils were epoxidized soybean (ESBO) oil (Elf Atochem Intl., PA), CMSBO #1, #2 and heat modified soybean oil (HMSBO; M–N viscosity).

HMSBO was prepared by thermal treatment of SBO under N_2 atmosphere in a closed reactor under constant stirring condition. Viscosity was carefully controlled to M–N grade according to Gardner scale.

Chemically modified soybean oils (CMSBO #1 and 2) were synthesized as part of a separate research project. In this procedure, the vegetable oil molecular structure was chemically modified in order to enhance its low temperature fluidity. All these oils were derived from SBO and maintained the basic triacylglycerol backbone. The pour point depressant (PPD) used was a mixture with the following composition: sunflower oil, mineral oil and undisclosed compounds (Lubrizol Corp., TM 7670).

2.2. Sub-ambient DSC procedures

DSC experiments were done on a TA Instruments (New Castle, DE) 2910 DSC-model 2100 with a computer-based controller. Before each experiment, the DSC cell was purged with low-pressure nitrogen gas. Typically 10 mg of the oil sample was accurately weighed in an open aluminum pan and placed in the DSC module with a similar empty pan as reference. The procedure involved rapidly heating the sample to 50 °C and then held under isothermal condition for 10 min. This helps in dissolving and homogenizing any waxy material present in the oil, which may inadvertently act as seed to accelerate wax crystal formation during cooling. The system was then cooled to −100 °C at a steady rate of 10 °C/min using liquid nitrogen as the cooling medium. The heat flow (W/g) versus temperature for each experiment was analyzed to determine wax appearance temperature (T_{C1}, °C) and onset temperature (T_{C2}, °C) corresponding to the second freezing peak (Pk-2). Average value of three independent measurements was taken in each case. The temperature repeatability was ±0.7 °C.

2.3. NMR experiments

Over the years, quantitative NMR spectroscopy has proved quite useful in elucidating the complex molecular structure of mineral [16–18] and vegetable oils [19,20]. ^{1}H NMR data of the vegetable oils were recorded in Fourier Transform mode on an AMX 400 MHz BRUKER machine at an observing frequency of 400 MHz using 5 mm dual nuclei probe. Deuterated

chloroform ($CDCl_3$) was used to prepare the sample solution (15%, w/v) containing 1% tetramethylsilane (TMS) as an internal standard. A pulse delay (D1) of 1 s, acquisition time (AQ) 6.8 s and pulse width (P1) 8.5 μs was used for 16 repeated scans (NS). Further details of the experiments are reported in an earlier publication [21].

2.4. Molecular modeling

A molecular modeling program (Spartan Pro) was used to build representative triacylglycerol molecules using a minimum energy calculation approach [22]. Modifications were made in the fatty acid chains by changing the oleic or linoleic acid moiety. Different triacylglycerol molecules were designed having both oleic chains, both linoleic chains and one each of oleic and linoleic chain on the two end side of 'tuning fork' structure, while the stem side had either oleic or linoleic chain. Geometrical and energy calculations on bond angle, planer distance between hydrogens in the same and adjacent chains, molecular energy associated with a sterically hindered geometry and conformation etc. were done on individual molecules.

2.5. Statistical method

Statistical analysis was used to develop correlations based on vegetable oil structural data obtained from ^{1}H NMR analysis and T_C determined from the DSC cooling curve. A professional version of Minitab® 12 statistical program was used in the current study. The program analyses individual NMR derived predictor variables one at a time and determines its influence on the T_C. The p-values were calculated and t-tests were done to identify variables that imparted maximum influence on T_C. The final model included those variables that showed the best correlation on the basis of their individual and collective influence on wax formation temperature.

3. Results and discussion

3.1. Analysis of sub-ambient DSC data

Fig. 1 shows the conventional DSC trace for HO saflr obtained by cooling the sample from +50 to −100 °C at the rate of 10 °C/min. Previous studies have shown that cooling rate can influence the shape of the curve as well as the corresponding temperature obtained [12]. Table 1 presents the wax appearance temperatures (T_{C1}, °C) of SBO corresponding to different cooling rates. It was observed that at a lower cooling rate (1–5 °C/min) the signal-to-noise ratio is low and the onset temperature is hard to estimate. The sensitivity of DSC measurement is directly related to heating and cooling rate used [23]. Therefore sensitivity of the instrument at a lower cooling rate can make the identification of wax appearance temperature difficult. The wax appearance onset temperature is relatively well defined from the base line at a higher cooling rate. With an increase in the rate of cooling, T_{C1} progressively shows lower value and the delta change is small compared to low cooling rate.

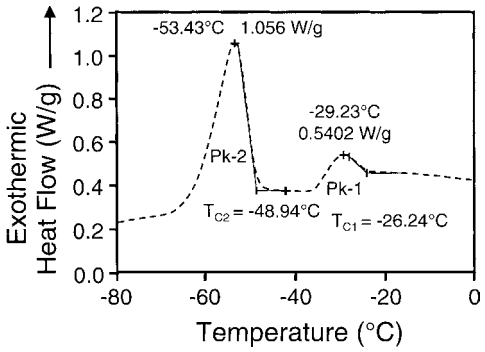

Fig. 1. Cooling curve of HO saflr oil at a cooling rate of 10 °C/min from +50 to −100 °C showing the exothermic peaks Pk-1 and Pk-2 and corresponding T_{C1} and T_{C2}.

Table 1
Wax appearance temperature of SBO at different cooling rates range = +50 to −50 °C, sample size: 9.9646 mg[a]

Base fluid	Cooling rate (°C/min)	Wax appearance temperature T_{C1} (°C)	Delta change in T_{C1} (°C)
SBO	1.0	−8.34	–
SBO	2.0	−9.29	11.39
SBO	3.0	−10.26	10.44
SBO	5.0	−11.07	7.89
SBO	7.0	−12.13	9.57
SBO	10.0	−13.16	8.49
SBO	12.0	−14.14	7.44
SBO	15.0	−14.52	2.68

[a] DSC data reported is the average value of duplicate experiments.

Table 2
Wax appearance temperature of vegetable oils from cooling curve; rate = 10 °C/min; range = +50 to −100 °C[a]

Vegetable oils	T_{C1} (°C)	T_{C2} (°C)
Cotton seed oil	−10.76	−35.04
Corn oil	−25.29	−43.44
Saflr oil	−24.16	−43.69
HO saflr oil	−26.24	−48.94
HL saflr oil	−21.28	−39.84
Sunflr oil	−14.92	−36.68
HO sunflr oil	−21.50	−45.76
SBO	−13.16	−35.48
HO soybean oil	−19.90	−45.41

[a] DSC data reported is the average value of three independent experiments. Repeatability of the data ±0.70; HO: high oleic, HL: high linoleic.

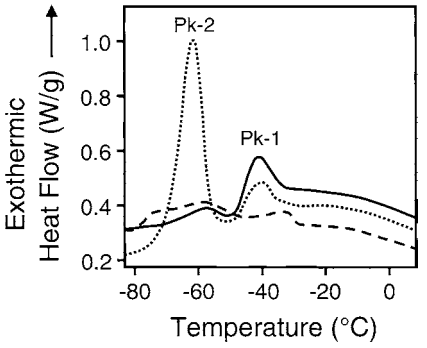

Fig. 2. Cooling curves of unmodified and genetically modified saflr oil. Saflr oil (—), HO saflr oil (· · ·) and HL saflr oil (– – –) at a cooling rate of 10 °C/min from +50 to −100 °C.

Therefore, an optimum rate of 10 °C/min has the advantage of being fast with greater data repeatability.

Except for ESBO, HMSBO and CMSBO #1 and 2, the cooling scan produced two distinct exothermic peaks (Pk-1 and Pk-2) for the rest of the vegetable oils (Fig. 1). Pk-1 was observed in the temperature range −10 to −30 °C while Pk-2 was between −35 and −50 °C (Table 2). T_{C1} and T_{C2} were defined as the temperature at the intersection of the line tangent on Pk-1 and Pk-2 respectively, with the baseline on the 'hot side' of the cooling curve. During the cooling process in vegetable oils, microcrystals start forming at temperature T_{C1}. Symmetrical packing of individual triacylglycerol molecules in bent conformation forms these crystals. This is represented on the DSC curve as the onset temperature of exothermal peak (Pk-1). On further cooling the solubilizing ability of oil is lowered and therefore it transforms from an increasingly viscous fluid to a solid material preceded by an onset temperature of freezing (T_{C2}) (Fig. 1).

Due to the presence of various triacylglycerol polymorphisms in crystal packing and the energy involved in low temperature crystallization, vegetable oils do not crystallize over a narrow temperature range ([24] and references therein). Instead, it is a slow continuous process when the microcrystalline structures initially formed becomes macro-crystalline and rapidly changes to a solid like consistency. Larger proportion of crystals formed at lower temperature is the unstable (α) polymorphic form. Separate work at different heating rate by other workers has shown [13] that the formation of this unstable material is almost entirely absent at slow cooling rate (0.1 °C/min), when only the polymorphic stable form (β) was observed.

The cooling curve of high oleic vegetable oils, unlike other oils, showed a relatively large exothermic Pk-2 as compared to Pk-1 (Fig. 2). The explanation for variation in wax appearance temperature of vegetable oil, consisting of a mixture of fatty acid moieties in the triacylglycerol molecule, cannot be based on the content of oleic acid alone (Fig. 3). Presence of other fatty acids (which act as solvent to stabilize the crystals formed during the cooling process) in vegetable oils may also influence crystallization. This fact can be appreciated by a close analysis of the data shown in Fig. 3 and Table 3. A comparison of the oleic content and T_{C1} of SBO, saflr and sunflr oil indicates

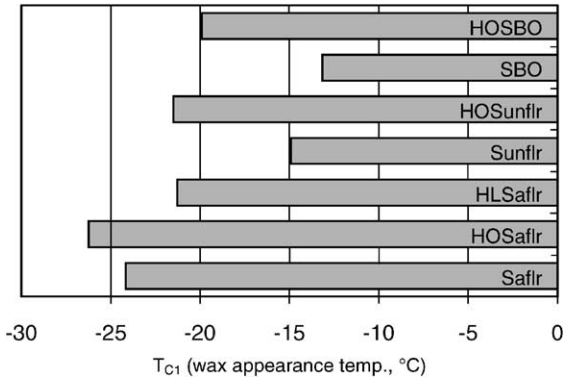

Fig. 3. Wax appearance temperatures (T_{C1}, °C) of unmodified and genetically modified vegetable oils using Cryo-DSC; cooling rate = 10 °C/min.

Table 3
Fatty acid composition of the vegetable oils by GC analysis[a]

Vegetable oils	Palmitic (16:0)	Stearic (18:0)	Oleic (18:1)	Linoleic (18:2)	Linoleic (18:3)
Saflr oil	6.4	2.5	17.9	73.2	–
HO saflr oil	4.6	2.2	77.5	13.2	–
HL saflr oil	6.7	2.6	14.6	75.2	–
Sunflr oil	6.1	5.3	21.4	66.4	–
HO sunflr oil	3.5	4.4	80.3	10.4	–
SBO	6.0	5.2	21.2	65.7	0.5
HO soybean oil	6.2	3.0	83.6	3.7	1.7

[a] Method: AACC method 58-18, 1993.

that wax appearance temperature increases with higher oleic content. Moreover, the relative distribution of palmitic (16:0) and stearic (18:0) acid has opposing effect with linoleic (18:2) acid moiety on the crystallization process. Similar argument can be extended for the comparison of genetically modified high oleic oils (Table 3, Fig. 3). Earlier work on pure triolein and trilinolein molecules has shown that the melting point of α and β forms of triolein is higher than trilinolein molecule [14]. Similar variation in the freezing onset temperature (T_{C2}) was observed for the other oils studied (Table 2).

Fig. 4 presents the wax appearance temperature of SBO and structurally modified soybean oil. In ESBO, C=C bond on the fatty acid chain was converted to epoxy ring. Gas chromatography and NMR data indicate a near complete removal of unsaturation in the molecule (unpublished results). It was observed that T_{C1} for ESBO was $-9.5\ ^{\circ}C$ compared to $-13.61\ ^{\circ}C$ in SBO. High T_{C1} for epoxy oil apparently resulted from

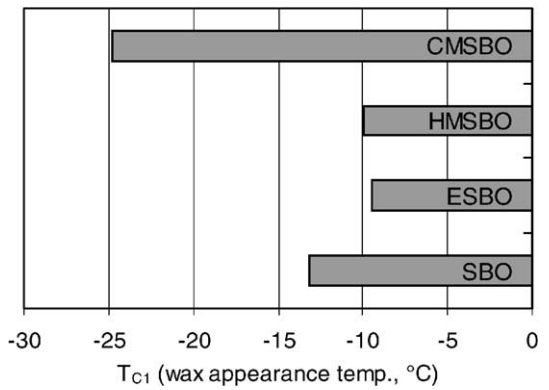

Fig. 4. Wax appearance temperature (T_{C1}, °C) of heat and CMSBO using Cryo-DSC; cooling rate = 10 °C/min.

low steric hindrance of epoxy ring during molecular stacking at low temperature. During this time microcrystalline waxy structures are formed and the oil becomes cloudy before rapid crystallization sets in. This phenomenon is also referred as the cloud point of the oil. It has been reported that the wax appearance temperature of oils can be correlated with their cloud point [12].

The T_{C1} of HMSBO ($-9.95\ ^{\circ}C$) was similar to ESBO. A significant lowering in T_{C1} was observed for CMSBO ($-24.77\ ^{\circ}C$) when compared to SBO, due to the presence of additional branching sites on the molecule. This highly branched structure prevented individual molecules to orient in a geometry that would allow them to stack in a low energy conformation to initiate crystal growth. Also, during such stacking process, the molecule has to spend an enormous amount of kinetic energy to overcome the steric interaction for packing during cooling process. This is often not the case and such molecules remain largely separate until they reach a very low temperature and actual crystallization sets in.

Fig. 5 presents the effect of a PPD on the wax appearance temperature of heat and CMSBOs. The function of PPD [25,26] in delaying wax formation is by physically disrupting the stacking process of the fork like structure during cooling. The PPDs are usually high molecular weight polymeric compounds that orient itself along the triacylglycerol molecule in such a way whereby they prevent the approach of a second molecule in close proximity to the first. This results in the formation of microcrystalline wax structures that are prevented from further agglomeration. It is observed that with an increase in the concentration of PPD there is a gradual decrease in the T_{C1} that reaches an optimum level at 4% v/v. The HMSBO

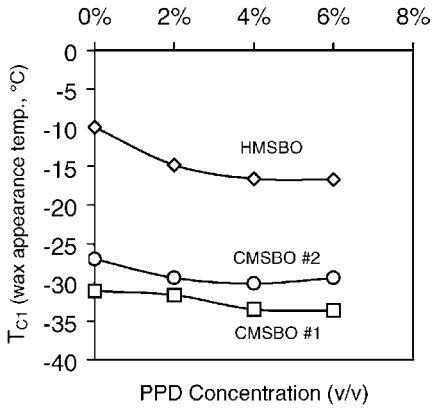

Fig. 5. Effect of PPD additive concentration on the lowering of T_{C1} in heat and CMSBOs.

registered a better response with PPD at a lower additive concentration as compared to the CMSBOs. However the CMSBO by itself showed a lower T_{C1} value as compared to HMSBO with different doses of additive. It is therefore evident from the above figure that low temperature fluidity of vegetable oils can be significantly improved by chemical modification of the vegetable oil structure before attempting additive response studies.

3.2. Analysis of molecular geometry

A modeling program (Spartan Pro) was used to build several representative triacylglycerol molecules with different fatty acid chains (mainly oleic and linoleic). Energy minimization approach was used to calculate the minimum energy molecular conformation and their three-dimensional orientations in space. The reported angular and distance measurements are from modeling results of entire molecule rather than individual atomic pairs. The energy encountered for the entire molecule was in the order of kJ/mol (not reported). The approach was to understand the mechanism of stacking in these molecules with different fatty acid chains during cooling process, in their bent conformation. It has been observed that the three-dimensional orientation of a molecule with 2-oleic, 2-linoleic or 1-oleic and 1-linoleic chains, making the 2-end side of the 'fork' structure, are different. This difference is mainly in the orientation of the $–CH_2–$ carbons separated by –C=C– bonds and

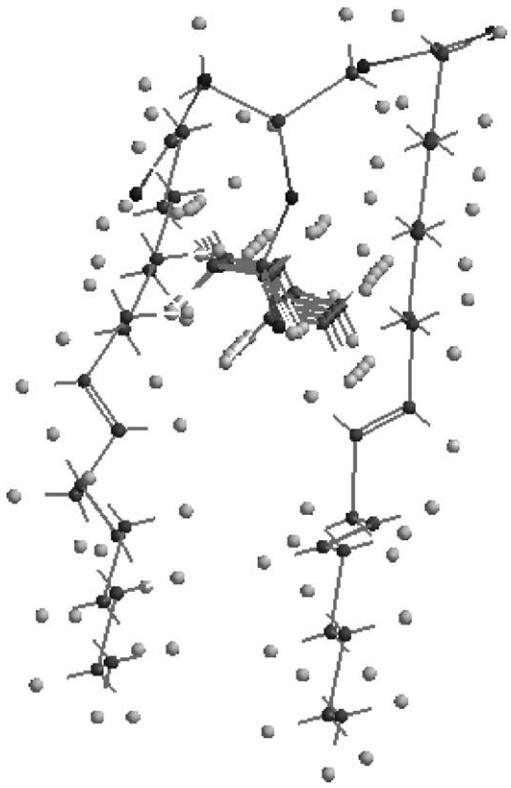

Fig. 6. Minimum energy conformation of oleic-linoleic acid pairs forming the 2-end side of 'tuning fork' structure with the third oleic chain forming the stem in the bent conformation.

the associated dihedral angles. In a triacylglycerol molecule with two adjacent oleic acid chains in the bent fork like structure, there is a 'zigzag' in the molecule due to the presence of a single C=C in the fatty acid. The two $–CH_2–$ planes are oriented differently and make an angle in the same chain but are more or less parallel to the adjacent chain. Similarly a molecule having an oleic and a linoleic chain at the 2-end side of the 'fork' structure would show the linoleic $–CH_2–$ plane's spatial orientation, which is significantly different from the oleic $–CH_2–$ planes (Fig. 6). This is however not the situation if both the chains are linoleic and adjacent in the bent fork conformation (Fig. 7). The presence of two C=C bonds separated by a bis-allylic $–CH_2–$ in each linoleic chain results in the $–CH_2–$ planes that are in staggered orientation to the adjacent chain, thus increasing the overall steric bulk when viewed along the chain length.

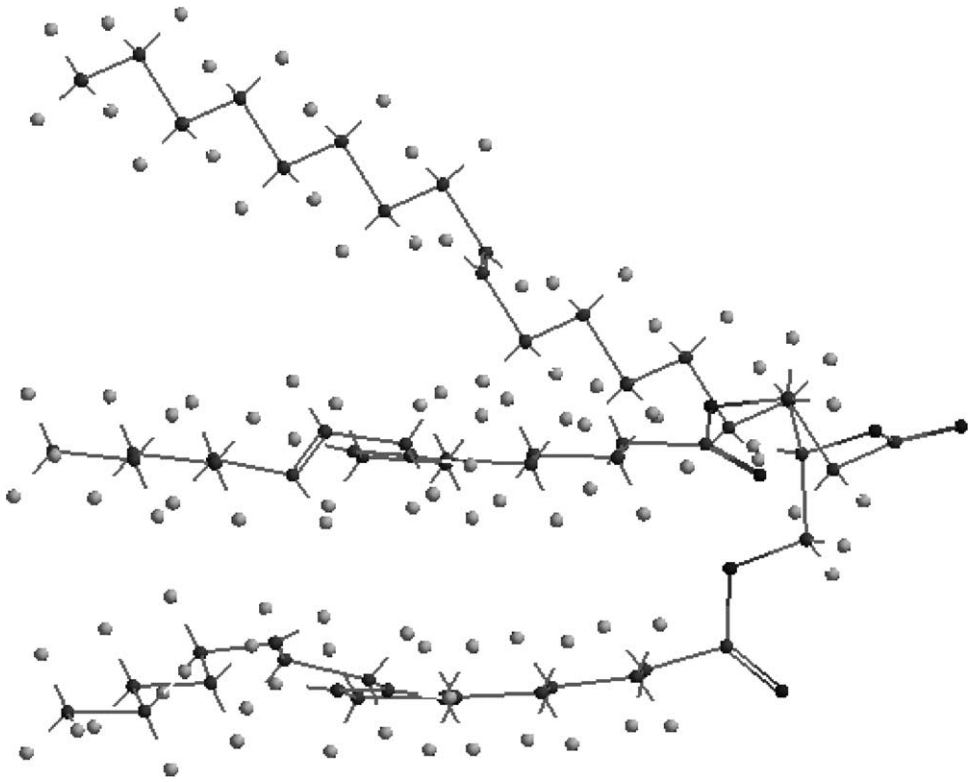

Fig. 7. Minimum energy conformation of 2-linoleic acid pairs forming the 2-end side of 'tuning fork' structure with the third oleic chain forming the stem in the bent conformation.

Table 4 presents the geometrical details of the triacylglycerol structures obtained using the modeling program. It is observed that the planer distance between two Hs on extreme ends of the same chain viewed along the chain length is 13.73 Å for two adjacent linoleic acid chains and 11.40 Å for two oleic chains. This distance between Hs gets reduced in the linoleic chain (10.77 Å) when a linoleic and oleic chain are adjacent. Due to the presence of two C=C bonds separated by a $–CH_2–$ (sp^3) carbon, there is a possibility of free rotation between the two $–CH_2–$ planes in the linoleic chain. This occurs in such a way that the planer spacing between two extreme Hs are reduced when they are adjacent to another oleic chain, with the latter being largely undisturbed sterically. Further the distance between closest approaches between two Hs on adjacent chains in the same plane varies between 2.55 and 3.75 Å in two adjacent linoleic chains. These distances between Hs are essentially unaltered in two oleic (2.62 Å) or oleic–linoleic (2.64 Å) combinations. Moreover the bis-allylic $–CH_2–Cs$ in two adjacent linoleic chains has a dihedral angle of 110.81°, significantly lower than the 115.32° in oleic–linoleic combination.

The steric hindrance experienced by two approaching molecules dictate condition for wax appearance to a fairly large extent. During the cooling process, the steric interaction of out-of-plane >C=O group and orientation of $–CH_2–$ planes in the fatty acid chains control the approach of the second molecule for a minimum energy conformation. Lesser the steric bulk of the fatty acid chain, faster and closer the approach of the second molecule, and higher the wax appearance temperature. This is a dynamic process and each time an additional molecule is stacked on the parent body, there is a slight steric adjustment to a new low energy conformation. It can therefore be concluded from the above table that a combination of planer distance between peripheral Hs and dihedral angle of individual molecule is important for the crystallization process.

Table 4
Calculated geometrical data obtained from energy-minimized structures of triacylglycerol molecules

	2-Linoleic acid chains[a]	2-Oleic acid chains[a]	Linoleic and oleic acid chains[a]
Distance between two Hs on extreme ends on the same chain[b]	13.73 Å	11.40 Å	Linoleic chain (L) = 10.77 Å, oleic chain (O) = 11.39 Å
Distance between two Hs on extreme ends on the same chain[b,c]	11.39 Å	–	–
Distance between two Hs on extreme ends on the same chain[b,d]	11.69 Å	11.69 Å	11.69 Å
Distance between the closest Hs on adjacent chains[b]	2.55–3.75 Å	2.62 Å	2.64 Å
$-CH_2-CH-CH_2-$	112.53°	112.51°	112.36°
$-CH_2-CH-O-$ (corresponding angle with the middle chain)	111.11°, 106.38°	109.23°, 106.60°	109.31°, 106.63°
$-O-CO-CH_2-$	109.41°	109.69°	L = 109.61°, O = 110.25°
$-O-CO-CH_2-$[d]	118.43°	118.78°	118.57°
$-CH_2-CH=CH-$	123.97°	127.39°	L = 127.40°, O = 127.50°
$=CH-CH_2-CH=$	110.81°	–	L = 115.32°
$-CH=CH-CH_2-$	124.24°	127.41°	L = 124.37°, O = 127.39°
$-CH_2-CH=CH-$[d]	123.90°	123.90°	123.89°

[a] Forming the 2-end side of the 'tuning fork' structure of triacylglycerol molecule.
[b] Perpendicular distance, viewed along the chain length of the fatty acid moiety.
[c] Linoleic acid chain formed the 1-end side of the 'tuning fork' structure.
[d] Oleic acid chain formed the 1-end side of the 'tuning fork' structure.

3.3. Analysis of statistical data

Quantitative NMR spectroscopy (mainly ^1H and ^{13}C) is now an integral part of various product and process optimization studies [27–30]. The technique is non-destructive and able to generate data at the molecular level for a more detailed and accurate approach to build statistical models [21,27]. This is in sharp contrast to the bulk physical property data earlier used in developing predictive models. Not surprisingly, such models fell short on various occasions, for now it is widely accepted that all the chemical and physical properties of base oils (both mineral and vegetable origin) are controlled by the relative distribution of their molecular structures ([16,21] and references therein). Table 5 presents the quantitative ^1H NMR data on different vegetable oils used in this study. The details of experiment protocol and peak assignments are discussed in a previous publication [21]. It was observed that vegetable oil low temperature crystallization behavior could be modeled by using certain ^1H NMR structural parameters as independent predictor variables. This is also supported from the molecular modeling of various triacylglycerol structures by energy minimization approach in the current study. There are however several limitations for using a single structural parameter to explain the wax appearance and freezing characteristics of vegetable oils due to the complexity of triacylglycerol structures and presence of various fatty acid moieties. The relative extent to which these structures affect T_C can be reliably determined by adopting a logical approach of multi-component statistical analysis of the NMR data.

Table 5
Quantitative ^1H NMR derived structural parameters of vegetable base oils[a]

Vegetable oils	Olefin proton (%)	Bis-allylic $-CH_2$ proton (%)	Allyl$-CH_2$ (%)
Cotton seed oil	8.80	2.83	8.76
Corn oil	10.04	3.38	10.51
Saflr oil	11.15	4.25	10.86
HO saflr oil	7.18	0.75	10.75
HL saflr oil	10.99	4.38	10.88
Sunflr oil	10.15	3.85	9.56
HO sunflr oil	6.90	0.62	10.55
SBO	10.26	4.13	10.40

[a] NMR data reported is the average value of three independent experiments. The repeatability of the data is ±0.2; HO: high oleic, HL: high linoleic.

The results from the multi-component analysis of T_{C1} yielded the following equation:

Wax appearance temperature,

$$T_{C1}\,(^{\circ}\mathrm{C}) = 91.2 - 15.8\,(\%\,\text{olefin}\,H) + 17.9\,(\%\,\text{bis-allylic}\,CH_2) - 1.5\,(\%\,\text{allylic}\,CH_2) \quad (1)$$

The equation has a coefficient of determination (R^2 adjusted) 0.93 and standard error of Y-estimate (σ_Y) 1.569. Analysis of the p-values and t-test of individual predictor variables suggest allylic CH_2 has a significant influence (R^2 adjusted = 0.57) while bis-allylic CH_2 the least on T_{C1}. However a combined olefin H and bis-allylic CH_2 has a tremendous impact on T_{C1} (R^2 adjusted = 0.92), which improved further when the third component was included in the final equation. Of the various other structural parameters available for vegetable oils [21,31], it is noticed that the extent and nature of unsaturation in the fatty acid chain along with their steric conformation plays the decisive role in determining T_{C1}. Fig. 8 presents the plot of experimental versus calculated data for T_{C1} for a total of eight different vegetable oil samples. The model (Eq. (1)) holds well for the determination of T_{C1} in the range 0 to −30 °C. Most of the vegetable oils (both unmodified and genetically modified) available would conveniently fall in this range.

Similar equation was derived for Pk-2 with the same set of predictor variables (Eq. (2)). It was observed that T_{C2} showed a better correlation with a lower σ_Y value of 0.669 and higher adjusted coefficient of determination 0.98. The p-value and t-test data on individual predictor variables show similar relative influence on T_{C2} but with higher percent accuracy in determination.

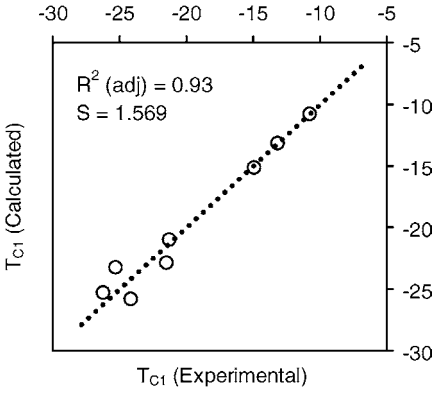

Fig. 8. Correlation plot of calculated versus experimentally observed T_{C1} data showing scatter of points on a 1:1 distribution. R^2 (adjusted) = 0.93; error of Y-estimate = 1.569.

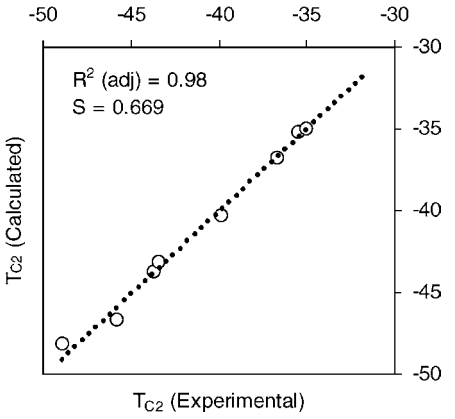

Fig. 9. Correlation plot of calculated versus experimentally observed T_{C2} data showing scatter of points on a 1:1 distribution. R^2 (adjusted) = 0.98; error of Y-estimate = 0.669.

Crystallization temperature,

$$T_{C2}\,(^{\circ}\mathrm{C}) = 32.9 - 10.9\,(\%\,\text{olefin}\,H) + 13.6\,(\%\,\text{bis-allylic}\,CH_2) - 1.2\,(\%\,\text{allylic}\,CH_2) \quad (2)$$

Fig. 9 presents the scatter of experimental versus calculated data on an ideal 1:1 correlation plot. The model is statistically valid in the temperature range −30 to −50 °C for the determination of T_{C2}.

4. Conclusions

DSC is an excellent method to measure the wax appearance and crystallization temperatures of vegetable oils. Due to the complexity of the vegetable oil composition with respect to their FA distribution, the situation is not as simple as pure triacylglycerol molecules. Moreover there is significant influence of the nature, relative abundance and orientation of C=C bonds on the wax appearance temperatures. Further, presence of other saturated short chain length FAs in vegetable oil structure is found to affect the crystallization process. Statistical analysis of ^{1}H NMR

derived vegetable oil structure support the influence of several predictor variables associated with FA unsaturation on the crystallization process. Distance and dihedral angle calculations on triacylglycerol structures using energy minimization molecular modeling approach were able to explain the relative crystallization tendency of vegetable oils in the bent 'fork' conformation.

References

[1] D. Chapman, Chem. Rev. 62 (1962) 433.
[2] C.W. Hoerr, F.R. Paulicka, J. Am. Chem. Soc. 45 (1968) 793.
[3] J.W. Hagemann, J.A. Rothfus, J. Am. Chem. Soc. 60 (1983) 1308.
[4] A.P. Bentz, B.G. Breidenbach, J. Am. Chem. Soc. 46 (1969) 60.
[5] V. Antila, J. Finn, Dairy Sci. 27 (1966) 1.
[6] C.K. Cross, J. Am. Chem. Soc. 47 (1970) 229.
[7] P. Claudy, J.M. Letoffe, B. Neff, B. Damin, Fuel 65 (1986) 861.
[8] P. Claudy, J.M. Letoffe, B. Chague, J. Orrit, Fuel 67 (1988) 58.
[9] F. Noel, Thermochim. Acta 4 (1972) 377.
[10] P. Redelius, Thermochim. Acta 85 (1985) 327.
[11] J.C. Hipeaux, M. Born, J.P. Durand, P. Claudy, J.M. Letoffe, Thermochim. Acta 348 (2000) 147.
[12] Z. Jiang, J.M. Hutchinson, C.T. Imrie, Fuel 80 (2001) 367.
[13] D.J. Cebula, K.W. Smith, J. Am. Chem. Soc. 68 (1991) 591.
[14] J.W. Hagemann, W.H. Tallent, K.E. Kolb, J. Am. Chem. Soc. 49 (1972) 118.
[15] J.W. Hagemann, J.A. Rothfus, J. Am. Chem. Soc. 60 (1983) 1123.
[16] A. Adhvaryu, J.M. Perez, I.D. Singh, Energy and Fuels 13 (1999) 493.
[17] A. Adhvaryu, J.M. Perez, I.D. Singh, O.S. Tyagi, Energy and Fuels 12 (1998) 1369.
[18] A. Adhvaryu, Y.K. Sharma, I.D. Singh, Fuel 78 (11) (1999) 1293.
[19] Y. Miyake, Y. Kazuhisa, N. Matsuzaki, J. Am. Oil. Chem. Soc. 75 (9) (1998) 1091.
[20] M.M. Bergana, T.W. Lee, J. Am. Oil. Chem. Soc. 73 (1996) 5.
[21] A. Adhvaryu, S.Z. Erhan, Z.S. Liu, J.M. Perez, Thermochim. Acta 364 (2000) 87.
[22] H.H. Rosenbrock, C. Storey, Computational Techniques for Chemical Engineers, Pergamon Press, Oxford, 1966, 64 pp.
[23] E.-L. Heino, Thermochim. Acta 114 (1987) 125.
[24] J.W. Hagemann, J.A. Rothfus, J. Am. Chem. Soc. 65 (4) (1988) 638.
[25] J. Denis, Lub. Sci. 1 (2) (1989) 103.
[26] J. Denis, J.P. Durand, Revue IFP 46 (5) (1991) 637.
[27] A. Adhvaryu, J.M. Perez, J.L. Duda, Tribol. Trans. 43 (2) (2000) 245.
[28] A.S. Sarpal, G.S. Kapur, S. Mukherjee, S.K. Jain, Energy and Fuels 11 (1997) 662.
[29] Y. Miyake, K. Yokomizo, N. Matsuzaki, J. Jpn. Oil. Chem. Soc. 47 (4) (1998) 333.
[30] C.M. Yang, A.A. Grey, M.C. Archer, W.R. Bruce, Nutr. Cancer 30 (1) (1998) 64.
[31] G. Vlahov, A.D. Shaw, D.B. Kell, J. Am. Chem. Soc. 76 (10) (1999) 1123.